Hindawi Publishing Corporation
Mathematical Problems in Engineering
Volume 2016, Article ID 7849175, 9 pages
http://dx.doi.org/10.1155/2016/7849175

Research Article

Characterization of Energy Availability in RF Energy Harvesting Networks

Daniela Oliveira[1] and Rodolfo Oliveira[1,2]

[1]*Instituto de Telecomunicações (IT), Avenida Rovisco Pais 1, 1049-001 Lisboa, Portugal*
[2]*Dep. de Eng. Electrotécnica, Faculdade de Ciências e Tecnologia (FCT), Universidade Nova de Lisboa, 2829-516 Costa da Caparica, Portugal*

Correspondence should be addressed to Rodolfo Oliveira; rado@fct.unl.pt

Received 12 June 2016; Accepted 8 September 2016

Academic Editor: Babak Shotorban

The multiple nodes forming a Radio Frequency (RF) Energy Harvesting Network (RF-EHN) have the capability of converting received electromagnetic RF signals in energy that can be used to power a network device (the energy harvester). Traditionally the RF signals are provided by high power transmitters (e.g., base stations) operating in the neighborhood of the harvesters. Admitting that the transmitters are spatially distributed according to a spatial Poisson process, we start by characterizing the distribution of the RF power received by an energy harvester node. Considering Gamma shadowing and Rayleigh fading, we show that the received RF power can be approximated by the sum of multiple Gamma distributions with different scale and shape parameters. Using the distribution of the received RF power, we derive the probability of a node having enough energy to transmit a packet after a given amount of charging time. The RF power distribution and the probability of a harvester having enough energy to transmit a packet are validated through simulation. The numerical results obtained with the proposed analysis are close to the ones obtained through simulation, which confirms the accuracy of the proposed analysis.

1. Introduction

The nodes forming a Radio Frequency (RF) Energy Harvesting Network (RF-EHN) have the capability of converting received electromagnetic RF signals in energy. The RF energy is converted by an energy harvester device, which is composed of an RF antenna, a band pass filter parametrized to the RF signals, and a rectifying circuit able to convert RF to DC power [1]. In this way the converted RF signals are used to charge a battery (usually a supercapacitor) with finite capacity [2]. The harvested energy accumulated in the battery can then be used to transmit a packet. However, the transmission is only possible if the level of accumulated energy is higher than a given threshold representing the minimum level of energy required to complete a packet transmission.

Recently, RF energy harvesting has attracted much attention and many efforts are being dedicated to develop innovative RF energy harvesting technologies as well as to investigate the performance of the networks formed by the harvesting devices. The RF energy harvesting literature dedicated to the efficient design of RF harvesting devices (see [3–7] for a few examples) is mainly focused on the minimization of the loss effects due to the RF-to-DC conversion and battery charging process. A different focus is also found in the literature, where the main goal is the study and characterization of RF-EHNs. Adopting a generic model for the RF energy harvesting devices, the goals are usually related with the scheduling of the harvesting devices in order to maximize the utilization of the RF energy and the frequency band constrained by specific throughput fairness policies [8]; the optimization of the harvester communication task to deal with the multiple tradeoffs associated with the physical and MAC layers [9, 10]; the characterization of the RF-EHN performance (throughput) and stability when RF energy harvesting is adopted [11]. Reference [12] investigates the performance (throughput) of a slotted Aloha random access wireless network consisting of two types of nodes: with unlimited energy supply and solely powered by an RF energy

harvesting circuit. To illustrate the design considerations of RF-based harvesting networks, [13] points out the primary challenges of implementing and operating such networks, including nondeterministic energy arrival patterns, energy harvesting mode selection, and energy-aware cooperation among base stations. Reference [14] adopts a stochastic geometry framework based on the Ginibre model to analyze the performance of self-sustainable communications over cellular networks with general fading channels. The expectation of the RF energy harvesting rate, the energy outage probability, and the transmission outage probability are evaluated over Nakagami-m fading channels.

RF-EHNs may also act as cognitive radio networks (CRNs), that is, using the spectrum in an opportunistic way without being licensed. Several works have explored these kinds of networks. Reference [15] provides an overview of the RF-EHNs including system architecture, RF energy harvesting techniques, and existing applications. The authors also explore various key design issues in the development of RF-EHNs, including cognitive radio networks. The work in [16] provides a comprehensive overview of recent development and challenges regarding the operation of cognitive radio networks powered by RF energy. Spectrum efficiency and energy efficiency are two critical issues in designing cognitive radio RF-EHNs. Reference [17] provides an overview of the RF-powered CRNs and discusses the challenges that arise for dynamic spectrum access in these networks. Focusing on the trade-off among spectrum sensing, data transmission, and RF energy harvesting, the authors discuss the dynamic channel selection problem in a multichannel RF-powered CRN. Reference [18] proposes a novel method for wireless networks coexisting where low-power mobiles in a secondary network, harvest ambient RF energy from transmissions by nearby active transmitters, while opportunistically accessing the spectrum licensed to the primary network. The authors analyze the transmission probability of harvesting terminals and the resulting spatial throughput. The optimal transmission power and terminals' density are also derived for maximizing the throughput. The work in [19] considers an RF-powered green cognitive radio network, where a central node harvests energy from ambient sources and wirelessly delivers random harvested energy to cognitive users. The work evaluates the performance of such a network, showing the feasibility of the behavior if the energy transmission rate is below a certain threshold. Reference [20] considers a network where the unlicensed users can perform channel access to transmit a packet or to harvest RF energy when the selected channel is idle or occupied by the primary user, respectively. The work is mainly focused on finding the channel access policy that maximizes the throughput of the secondary user. Reference [21] analyzes an energy harvesting-based cognitive radio system to find the optimal spectrum sensing time, which maximizes the harvested energy. The work in [22] analyzes a cognitive and energy harvesting-based device-to-device (D2D) communication in cellular networks. The authors employ tools from stochastic geometry to evaluate the performance of the proposed communication system model with general path-loss exponent in terms of outage probability for D2D and cellular users. One of the work conclusions is that energy harvesting can be a reliable alternative to power cognitive D2D transmitters, while achieving acceptable performance.

In this work we are particularly focused on the characterization of the RF power received by each harvester and its impact in terms of the probability of accumulating enough energy to transmit a packet. A generalized radio propagation environment is considered. Assuming that the sources of high power RF signals (e.g., base stations) are distributed according to a spatial Poisson process, we characterize the distribution of the received RF power from the multiple transmitters. Path loss, shadowing, and fading effects are considered. The distribution of the RF power is then used to derive the probability of a harvester node having enough energy to transmit a packet after a given period of time. A soft computational model (Gaussian approach) and a more complex model (non-Gaussian approach) are presented to compute the probability of a harvester node having enough energy to transmit. These are the main contributions of the paper. Considering multiple spatial and propagation scenarios, we validate the distribution of the RF power and the probability of a harvester have enough energy to transmit a packet. The numerical results obtained with the proposed analysis are close to the ones obtained through simulation, which confirms the accuracy of the proposed analysis. In this way, we provide a characterization of the battery charging time considering innovative assumptions, including the spatial distribution of the RF transmitters, the propagation effects, and the losses associated with the RF-to-DC conversion and battery charging process. The proposed model can thus be adopted to determine the probability of a harvester accumulating enough energy after a given period of time, which is a determinant condition to compute the throughput of RF-EHNs. As far as we known, this is the first work to derive such a probability when the multiple RF signals received by the harvesters are differently affected by multiple propagation effects.

The rest of the paper is organized as follows. The system description is presented in Section 2. The characterization of the received RF power is characterized in Section 3. Section 4 derives the probability of accumulating enough energy to transmit a packet through the Gaussian and non-Gaussian approaches. Finally, validation results are presented in Section 5 and conclusions are drawn in Section 6.

2. System Description

This work considers a RF energy harvesting network, where each node accumulates energy from the base stations and other RF transmitters located in the neighborhood. A harvester node is able to initiate a packet transmission whenever the level of accumulated energy is above a transmission threshold.

2.1. Spatial Distribution of the RF Transmitters. We consider the scenario illustrated in Figure 1, where the node N_H (the harvester node) accumulates energy from the transmitters that might be located in the area $A = \pi((R_o^L)^2 - (R_i^1)^2)$. The

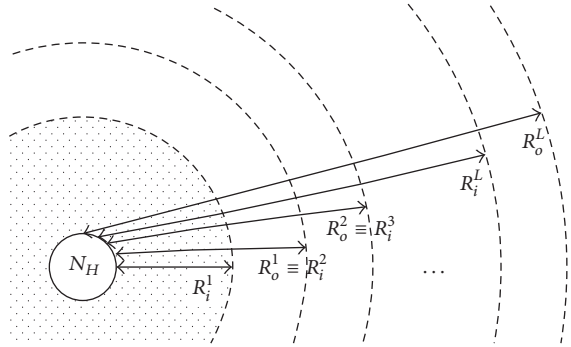

FIGURE 1: The harvester node N_H receives RF power from the transmitters located in the area $A = \pi((R_o^L)^2 - (R_i^1)^2)$.

area A can be obtained via calculus by dividing the annulus up into an infinite number of annuli of infinitesimal width $d\chi$ and area $2\pi\chi\, d\chi$ and then integrating from $\chi = R_i^1$ to $\chi = R_o^L$; that is; $A = \int_{R_i^1}^{R_o^L} 2\pi\chi\, d\chi$. Using the Riemann sum, A can be approximated by the sum of the area of a finite number (L) of annuli of width ρ,

$$A \approx \sum_{l=1}^{L} A_l, \tag{1}$$

where $A_l = \pi((R_o^l)^2 - (R_i^l)^2)$ denotes the area of the annulus l. $R_o^l = (R_i^1 + l\rho)$ and $R_i^l = (R_i^1 + (l-1)\rho)$ represent the radius of the larger and smaller circles of the annulus l, respectively.

The number of transmitters located in a specific annulus $l \in \{1, \ldots, L\}$, represented by the random variable (RV) X_l, is approximated by a Poisson process, being its Probability Mass Function (PMF) for a finite domain given by [23]

$$P(X_l = k) = \frac{\left((\beta_l A_l)^k / k!\right) e^{-\beta_l A_l}}{\sum_{i=0}^{n} \left((\beta_l A_l)^i / i!\right) e^{-\beta_l A_l}}, \quad k = 0, 1, \ldots, n, \tag{2}$$

where β_l is the spatial density of the RF nodes transmitting in the annulus and n is the total number of mobile nodes.

2.2. Propagation Assumptions. We consider that the RF power I_i received by the harvester N_H from the RF transmitter i is given by

$$I_i = P_{Tx} \psi_i r_l^{-\alpha}, \tag{3}$$

where P_{Tx} is the transmitted power level of the ith RF transmitter ($P_{Tx} = 20 \times 10^3$ mW is assumed for each node) and ψ_i is an instant value of the fading and shadowing gain observed in the channel between the receiver N_H and the transmitter node i. r_l represents the distance between the ith transmitter and the receiver. The values r_l and ψ_i represent instant values of the random variables R_l and Ψ_i, respectively. α represents the path-loss coefficient.

The PDF of R_l can be written as the ratio between the perimeter of the circle with radius x and the total area A_l, being represented as follows:

$$f_{R_l}(x) = \begin{cases} \dfrac{2\pi x}{A_l} & R_i^l < x < R_o^l, \\ 0, & \text{otherwise.} \end{cases} \tag{4}$$

To characterize the distribution of Ψ_i the small-scale fading (fast fading) and shadowing (slow fading) effects must be considered. The amplitude of the small-scale fading effect is assumed to be distributed according to a Rayleigh distribution, which is represented by

$$f_\zeta(x) = \frac{x}{\sigma_\zeta^2} e^{-x^2/2\sigma_\zeta^2}, \tag{5}$$

where x is the envelope amplitude of the received signal. $2\sigma_\zeta^2$ is the mean power of the multipath received signal. $2\sigma_\zeta^2 = 1$ is adopted in this work to consider the case of normalized power.

Regarding the shadowing effect, we have assumed that it follows a log-normal distribution

$$f_\xi(x) = \frac{1}{\sqrt{2\pi}\sigma_\xi x} e^{-(\ln(x)-\mu)^2/2\sigma_\xi^2}, \tag{6}$$

where σ_ξ is the shadow standard deviation when $\mu = 0$. The standard deviation is usually expressed in decibels and is given by $\sigma_{\xi\text{dB}} = 10\sigma_\xi / \ln(10)$. For $\sigma_\xi \to 0$, no shadowing results. Although (6) appears to be a simple expression, it is often inconvenient when further analyses are required. Consequently, [24] has shown that the log-normal distribution can be accurately approximated by a Gamma distribution, defined by

$$f_\xi(x) \approx \frac{1}{\Gamma(\vartheta)} \left(\frac{\vartheta}{\omega_s}\right)^{\vartheta} x^{\vartheta-1} e^{-x(\vartheta/\omega_s)}, \tag{7}$$

where ϑ is equal to $1/(e^{\sigma_\xi^2} - 1)$ and ω_s is equal to $e^\mu \sqrt{(\vartheta+1)/\vartheta}$. $\Gamma(\cdot)$ represents the Gamma function.

The probability density function of Ψ_i is thus represented by

$$f_{\Psi_i}(x) \approx f_{\zeta^2}(x) \cdot f_\xi(x) \approx \frac{2}{\Gamma(\vartheta)} \left(\frac{\vartheta}{\omega_s}\right)^{(\vartheta+1)/2} x^{(\vartheta-1)/2} K_{\vartheta-1}\left(\sqrt{\frac{4\vartheta x}{\omega_s}}\right), \tag{8}$$

which is the Generalized-K distribution, where $K_{\vartheta-1}(\cdot)$ is the modified Bessel function of the second kind.

Due to the analytical difficulties of the Generalized-K distribution, an approximation of the PDF (8) by a more tractable PDF is needed. Reference [25] provides an approximation of the Generalized-K distribution by using the moment matching method to determine the parameters of the approximated Gamma distribution. With this method,

[25] shows that the scale (θ_ψ) and shape (k_ψ) parameters of the Gamma distribution are given by

$$\theta_\psi = \left(\frac{2(\vartheta+1)}{\vartheta} - 1\right)\omega_s, \tag{9}$$

$$k_\psi = \frac{1}{2(\vartheta+1)/\vartheta - 1}, \tag{10}$$

respectively.

3. RF Received Power

3.1. RF Received Power due to the Transmitters Located within the Annulus l. The amount of RF power received by the harvester node N_H located in the centre of an annulus l is given by

$$\Sigma = \sum_{i=1}^{n_l} I_i, \tag{11}$$

where I_i is the RF power received from the ith transmitter and n_l is the total number of transmitters in the annulus l.

Let $M_I^i(s)$ represent the MGF of the ith transmitter located within the annulus ($i = 1, \ldots, n_l$) given by

$$M_I^i(s) = \mathrm{E}_{I_i}\left[e^{sI_i}\right] = \mathrm{E}_{\Psi_i}\left[\mathrm{E}_{R_l}\left[e^{sI_i}\right]\right]. \tag{12}$$

Using the PDF of the distance given in (4) and the PDF of the small-scale fading and shadowing effects in (8), the MGF of the power received by the node N_H from the ith transmitter in (12) can be written as follows:

$$M_I^i(s) = \int_0^{+\infty}\int_{R_i^l}^{R_o^l} e^{sI_i} f_{R_l}(r_l)\, f_{\Psi_i}(\psi_i)\, dr_l\, d\psi_i, \tag{13}$$

which using (3), (9), (10), and (4) can be simplified to

$$M_I^i(s) = \frac{2\pi}{A_l\left(2+k_\psi\alpha\right)\left(P_{Tx}\theta_\psi s\right)^{k_\psi}} \cdot \left(\left(R_o^l\right)^{2+k_\psi\alpha}\varrho\left(R_o^l\right) - \left(R_i^l\right)^{2+k_\psi\alpha}\varrho\left(R_i^l\right)\right), \tag{14}$$

where $\varrho(x) = {}_2\mathrm{F}_1(k_\psi, k_\psi + 2/\alpha, 1 + k_\psi + 2/\alpha, -x^\alpha/P_{Tx}\theta_\psi s)$ and ${}_2\mathrm{F}_1$ represents the Gauss Hypergeometric function [26].

Departing from the fact that the individual power I_i is independent and identically distributed when compared to the other transmitters, the PDF of the aggregate RF power I given a total of k active transmitters is the convolution of the PDFs of each I_i. Following this rationale, the MGF of I is given by

$$M_{I/k}(s) = M_I^1(s) \times M_I^2(s) \times \cdots \times M_I^k(s) = \left(M_I^i(s)\right)^k. \tag{15}$$

Using the law of total probability, the PDF of the RF power I can be written as

$$f_I(j) = \sum_{k=0}^{n} f_I(j \mid X_l = k)\,\mathrm{P}(X_l = k), \tag{16}$$

leading to the MGF of the aggregate power, I, which can be written as

$$\mathrm{E}\left[e^{sI}\right] = \sum_{k=0}^{n}\mathrm{P}(X_l = k)\int_{-\infty}^{+\infty} e^{sj} f_I(j \mid X_l = k)\, dj = \sum_{k=0}^{n}\mathrm{P}(X_l = k)\, M_{I/k}(s). \tag{17}$$

Using (15), the MGF of I is given as follows:

$$\mathrm{E}\left[e^{sI}\right] = \sum_{k=0}^{n}\mathrm{P}(X_l = k)\, e^{k\ln(M_I^i(s))}. \tag{18}$$

Using the MGF of the Poisson distribution in (18), the MGF of I is finally given by

$$\mathrm{E}\left[e^{sI}\right] = e^{\beta_l A_l (M_I^i(s)-1)}. \tag{19}$$

The first- and second-order statistics of the aggregate RF power received by N_H from the transmitters located within the annulus l are an important tool. E[I], the expected value of the aggregate RF power, can be determined by using the Law of Total Expectation. It can be shown that

$$\mathrm{E}[I] = \mathrm{E}\left[\mathrm{E}[I \mid X_l]\right] = 2\pi\beta_l P_{Tx}\sqrt{e^{\sigma_\xi^2}}\left(\frac{\left(R_o^l\right)^{2-\alpha} - \left(R_i^l\right)^{2-\alpha}}{2-\alpha}\right). \tag{20}$$

Making similar use of the Law of Total Variance, the variance of the aggregate RF power can be described as

$$\mathrm{Var}[I] = \mathrm{Var}[I_i]\,\mathrm{E}[X_l] + \mathrm{E}[I_i]^2\,\mathrm{Var}[X_l]. \tag{21}$$

Since X_l is given by a Poisson distribution (with mean $\beta_l A_l$), the variance of the RF power is given as follows:

$$\mathrm{Var}[I] = \beta_l A_l\left(\frac{\partial^2 M_I^i(0)}{\partial s^2}\right) = \pi\beta_l P_{Tx}^2 k_\psi\theta_\psi^2\left(1+k_\psi\right)\left(\frac{\left(R_o^l\right)^{2-2\alpha} - \left(R_i^l\right)^{2-2\alpha}}{1-\alpha}\right). \tag{22}$$

The first and second moments can be matched with the respective moments of a given distribution to obtain a closed-form approximation for the aggregate received RF power. As shown in [27], the aggregate RF power due to path loss, fast fading, and shadowing effect can be approximated by a Gamma distribution. Consequently, the shape and the scale parameters of the Gamma distribution, denoted by k_l and θ_l, are, respectively, given by

$$k_l \approx \frac{\mathrm{E}[I]^2}{\mathrm{Var}[I]}, \tag{23}$$

$$\theta_l \approx \frac{\mathrm{Var}[I]}{\mathrm{E}[I]}. \tag{24}$$

3.2. RF Received Power due to the Transmitters Located within L Annuli. As shown in the previous subsection, the RF power I received from the transmitters located within the lth annulus is approximated by a Gamma distribution, with MGF $M_I^l(s) = (1-\theta_l s)^{-k_l}$. Since the annulus of width $R_o^L - R_i^1$ where the transmitters are located can be expressed as a summation of L annuli of width ρ, the MGF of the aggregate power received from the transmitters located within the L annuli is given by

$$M_{I_{\text{agg}}}(s) = \prod_{l=1}^{L} (1-\theta_l s)^{-k_l}. \tag{25}$$

Finally the expectation of the aggregate RF power can be computed as follows:

$$\mathrm{E}\left[I_{\text{agg}}\right] = \frac{\partial M_{I_{\text{agg}}}(0)}{\partial s}. \tag{26}$$

3.3. Distribution of the Aggregate RF Power. The aggregate RF power may be stated as being the summation of the L individual aggregated RF powers received from the transmitters located within each annulus. Expressions for the PDF and the CDF of the summation of L independent Gamma random variables were initially derived by Mathai in [28]. Those were simplified in [29] in order to be computed more efficiently.

Let $\{Z_l\}_{l=1}^{L}$ be independent but not necessarily identically distributed Gamma variables with parameters k_l (shape) and θ_l (scale). The PDF of the aggregate RF power is written as $I_{\text{agg}} = \sum_{l=1}^{L} Z_l$, which can be approximated by [29]

$$f_{I_{\text{agg}}}(x) \approx \prod_{l=1}^{L}\left(\frac{\theta_1}{\theta_l}\right)^{k_l} \sum_{w=0}^{+\infty} \frac{\delta_w x^{(\sum_{l=1}^{L} k_l + w - 1)} \exp\left(-x/\theta_1\right)}{\theta_1^{(\sum_{l=1}^{L} k_l + w)} \Gamma\left(\sum_{l=1}^{L} k_l + w\right)}, \tag{27}$$

where $\theta_1 = \min_l\{\theta_l\}$, δ_w coefficients are computed recursively, $\delta_{w+1} = (1/(w+1)) \sum_{i=1}^{w+1} [\sum_{l=1}^{L} k_l (1-\theta_1/\theta_l)^i] \delta_{w+1-i}$, and $\delta_0 = 1$. $\Gamma(\cdot)$ is the Gamma function. Finally, the CDF of I_{agg}, $F_{I_{\text{agg}}}(x) = \int_{-\infty}^{x} f_{I_{\text{agg}}}(z)dz$, is computed as follows [29]:

$$F_{I_{\text{agg}}}(x) \approx \prod_{l=1}^{L}\left(\frac{\theta_1}{\theta_l}\right)^{k_l} \sum_{w=0}^{\infty} \frac{\delta_w}{\theta_1^{\sum_{l=1}^{L} k_l + w} \Gamma\left(\sum_{l=1}^{L} k_l + w\right)} \times \int_0^x z^{\sum_{l=1}^{L} k_l + w - 1} \exp\left(-\frac{z}{\theta_1}\right) dz. \tag{28}$$

4. Probability of Transmission

4.1. Gaussian Approach. Departing from the fact that the RF power received from the transmitters located in the annulus l can be approximated by a Gamma distribution,

$$\text{Gamma}\left(k_l, \theta_l\right), \tag{29}$$

with k_l and θ_l given by (23) and (24), respectively, the envelope signal (amplitude) received from the transmitters is given by the square root of a Gamma distributed random variable, which is given by a Generalized Gamma distribution with the following parameters,

$$A_I^l = \mathcal{GG}\left(\sqrt{\theta_l}, 2k_l, 2\right). \tag{30}$$

Since a Gamma distribution, with shape k_l and scale θ_l, is the sum of k Exponential $(1/\theta_l)$ distributions, using the Central Limit Theorem (CLT), when k_l is large, the Generalized Gamma distribution can be approximated by a normal distribution [30]. In these conditions the amplitude of the aggregate signals received by the harvester N_H from the transmitters located in the annulus l can be also approximated by a normal distribution represented by

$$A_I^l \approx \mathcal{N}\left(\mu_{A_I^l}, \sigma_{A_I^l}^2\right) \approx \mathcal{N}\left(\eta\sqrt{\theta_l}\frac{\Gamma\left(k_l + 1/2\right)}{\Gamma\left(k_l\right)}, \eta^2\theta_l\left(\frac{\Gamma\left(k_l+1\right)}{\Gamma\left(k_l\right)} - \frac{\Gamma\left(k_l+1/2\right)^2}{\Gamma\left(k_l\right)^2}\right)\right), \tag{31}$$

where the loss factor $0 < \eta < 1$ represents the losses associated with the RF-to-DC conversion and battery charging efficiency.

During the battery charging period, the received power $(A_I^l)^2$ is accumulated in a discrete period of time Δ_t. The amount of energy stored in the battery of the harvester node during n_t time intervals is given by

$$\epsilon_l = \Delta_t \sum_{n=1}^{n_t} \left|A_I^l\right|^2. \tag{32}$$

Considering the unit variance random variable $\epsilon_l' = \sum_{n=1}^{n_t} |A_I^l/\sigma_{A_I^l}|^2$, with

$$\epsilon_l = \epsilon_l' \times \sigma_{A_I^l}^2, \tag{33}$$

and considering $\Delta_t = 1$ for the sake of simplicity, ϵ_l' follows a noncentral Chi-squared distribution with noncentrality parameter $\lambda_l = \sum_{k=1}^{n_t} (\mu_{A_I^l}/\sigma_{A_I^l})^2$. When n_t is large enough, it is possible to use the Central Limit Theorem to approximate the Chi-square distribution to a Gaussian distribution [31], and the following approximation holds

$$\epsilon_l' \approx \mathcal{N}\left(n_t + \lambda_l, 2\left(n_t + 2\lambda_l\right)\right). \tag{34}$$

Using (33), the energy accumulated in the battery of the harvester node N_H due to the transmitters located in the annulus l follows the following Gaussian distribution:

$$\epsilon_l \approx \mathcal{N}\left(\mu_l, \sigma_l^2\right) \approx \mathcal{N}\left(\sigma_{A_I^l}^2\left(n_t + \lambda_l\right), \sigma_{A_I^l}^4\left[2\left(n_t + 2\lambda_l\right)\right]\right). \tag{35}$$

Because L annuli are considered, the energy accumulated in the battery of the harvester node N_H due to the transmitters located in the L annuli is given by

$$\epsilon = \sum_{l=1}^{L} \epsilon_l, \tag{36}$$

and ϵ follows the following distribution

$$\epsilon \approx \mathcal{N}\left(\sum_{l=1}^{L}\mu_l, \sum_{l=1}^{L}\sigma_l^2\right) \approx \mathcal{N}\left(\mu_{\Sigma_L}, \sigma_{\Sigma_L}^2\right). \tag{37}$$

Therefore, denoting γ as the level of battery charge (accumulated energy) required to transmit a packet, the probability of reaching a γ level of accumulated energy after n_t units of time is given by

$$P_C = \mathcal{Q}\left(\frac{\gamma - \mu_{\Sigma_L}}{\sigma_{\Sigma_L}^2}\right), \tag{38}$$

where $\mathcal{Q}(x) = (1/\sqrt{2\pi})\int_x^\infty e^{-u^2/2}du$ is the complementary distribution function of the standard normal.

4.2. Non-Gaussian Approach. In the last subsection the CLT was used to approximate the amplitude of the aggregate signals received by the harvester N_H from the transmitters located in the annulus l, A_I^l, as represented in (31). However, when k_l is small, the CLT does not hold and, consequently, the Gaussian approach is not valid. In what follows we present a formulation when CLT does not hold. While the formulation is more computationally complex, it exhibits higher accuracy for low k_l values.

Departing from the MGF in (25), the Characteristic Function (CF) of the RF power received from the annulus l is written as

$$\varphi_l(t) = \prod_{l=1}^{L}\left(1 - \eta\theta_l it\right)^{k_l}, \tag{39}$$

where $0 < \eta < 1$ is the loss factor. When the aggregate power from the L annuli is considered the CF is written as follows:

$$\varphi_{I_{\text{agg}}}(t) = \prod_{l=1}^{L}\left(1 - \eta\theta_l it\right)^{k_l}. \tag{40}$$

Because the amount of energy received in n_t samples is expressed as

$$\epsilon = \sum_{n=1}^{n_t} I_{\text{agg}}(t), \tag{41}$$

the CF of ϵ is as follows:

$$\begin{aligned}\varphi_\epsilon(t) &= \prod_{b=1}^{n_t}\left(\varphi_{I_{\text{agg}}}(t)\right) = \prod_{b=1}^{n_t}\left(\prod_{l=1}^{L}\left(1 - \eta\theta_l it\right)^{\kappa_l}\right) \\ &= \prod_{l=1}^{L}\left[\left(1 - \eta\theta_l it\right)^{\kappa_l}\right]^{n_t}.\end{aligned} \tag{42}$$

Table 1: Parameters adopted in the validation and simulations.

ρ	$\{400, 200, 100, 4\}$ m
L	$\{2, 4, 100\}$
β_l	$\{1, 2, 3, 4\} \times 10^{-7}$ nodes/m^2
α	2
η	0.5
Δ_t	1 minute
R_i^1	10 m
R_o^L	410 m
P_{Tx}	20 W
$\sigma_{\xi\text{dB}}$	4.5 dB
γ	10 mAh
n_t	20

Using the Fourier Transform, the PDF of ϵ is written as

$$f_\epsilon(x) = \frac{1}{2\pi}\int_{-\infty}^{+\infty} e^{-itx}\varphi_\epsilon(t)\,dt. \tag{43}$$

Again, the probability of reaching a γ level of accumulated energy after n_t units of time is given by

$$P_C(\epsilon > \gamma) = 1 - P(\epsilon \le \gamma) = 1 - \int_{-\infty}^{\gamma} f_\epsilon(x)\,dx. \tag{44}$$

5. Validation Results

This section describes a set of simulations and numerical results to validate the analytical methodology proposed in the paper. The simulated scenario considered a spatial circular area A as described in Section 2 with $R_i^1 = 10$ m and $R_o^L = 410$ m. The multiple nodes were spread over the area A according to the spatial Poisson process and 4 different spatial densities were simulated, $\beta_l = \{1, 2, 3, 4\} \times 10^{-4}$ nodes/m^2. In each simulation the RF propagation scenario described in Section 2 was parametrized with $\alpha = 2$, and $\sigma_{\xi\text{dB}} = 4.5$ dB. Finally, we have considered the battery operation voltage equal to 1 V, the loss factor $\eta = 0.5$, and the required energy threshold to transmit a packet (γ) equal to 10 mAh. The parameters used in the validation are summarized in Table 1.

The first results, presented in Figure 2, compare the CDF of the RF received power computed with (28). The simulated results were obtained for the spatial density value $\beta_l = 1 \times 10^{-4}$. In the model, a different number ($L = \{2, 4, 100\}$) of annuli were adopted to compute the model and compare the accuracy of the model for different number of annuli. As can be seen, the accuracy of the model increases with the number of annuli considered in the model. This is because as more annuli are considered for the same circular area $A = \pi((R_o^L)^2 - (R_i^1)^2)$, the width of each annulus ρ decreases, leading to a more accurate value of the mean and variance (E$[I]$ and Var$[I]$, resp.) of the RF power received from the transmitters located in a single annuli. This fact increases the accuracy of the conditions in (23) and (24), leading to a more accurate characterization of the distribution of the received RF power. From the results plotted in Figure 2, we observe that for $L = 100$ the numerical results are close to the results

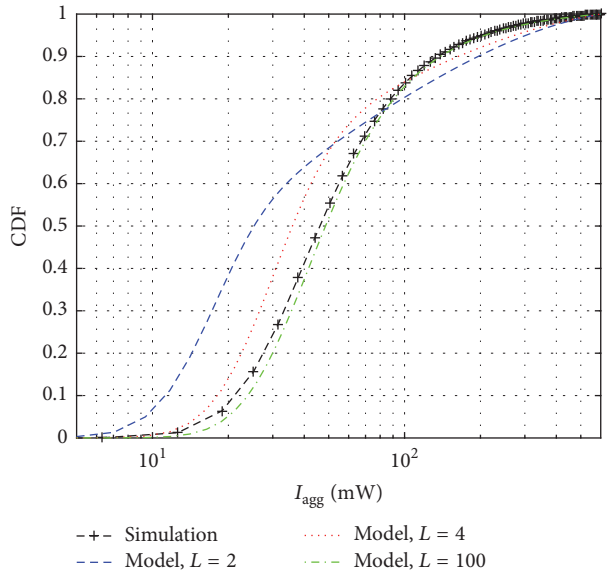

FIGURE 2: CDF of the RF power received by the node N_H from the transmitters located in the area $A = \pi((R_o^L)^2 - (R_i^1)^2)$.

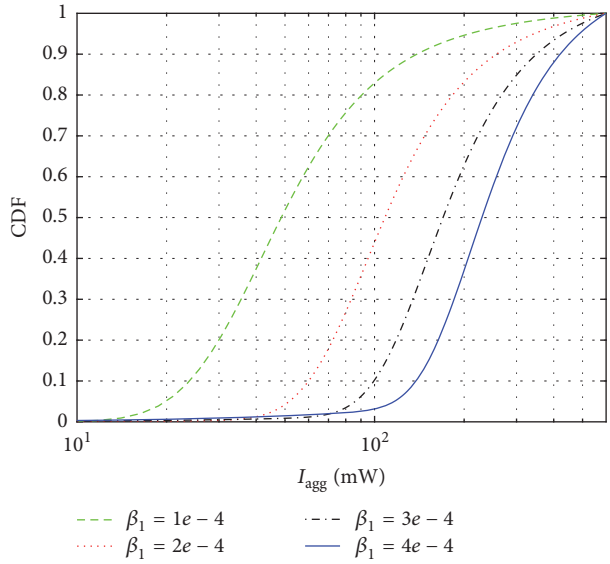

FIGURE 3: CDF of the RF power received by the node N_H considering different densities of transmitters (β_l in nodes per square meter) located in the area $A = \pi((R_o^L)^2 - (R_i^1)^2)$.

obtained through simulation, confirming the accuracy of the proposed model.

The numerical results presented in Figure 3 compare the CDF of the RF received power (computed with (28)) for different spatial density values ($\beta_l = \{1 \times 10^{-4}, 2 \times 10^{-4}, 3 \times 10^{-4}, 4 \times 10^{-4}\}$). The numerical results were obtained considering $L = 100$ (consequently $\rho = 4$). As expected, the results confirm that the average of the RF power received by the harvester increases with the spatial density of the transmitters.

In Figure 4 we compare the probability of having enough energy accumulated in the harvester battery to transmit a

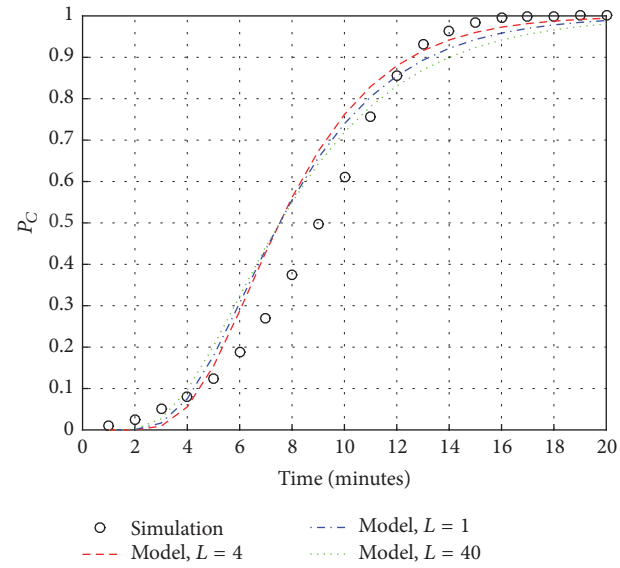

FIGURE 4: Gaussian approach model: probability of having enough energy accumulated in the harvester battery to transmit a packet (P_C) for different density $\beta = 4 \times 10^{-4}$ of transmitters (β_l in nodes per square meter) located in the area $A = \pi((R_o^L)^2 - (R_i^1)^2)$.

packet (P_C). The probability was computed using (38); that is, the Gaussian approach was adopted. The simulated values were obtained for the spatial density value $\beta_l = 4 \times 10^{-4}$ nodes/m^2. The charging threshold γ was defined to 10 mAh and we have considered a battery voltage of 1 V. The model was computed for $L = 1$ ($\rho = 400$), $L = 2$ ($\rho = 200$), and $L = 40$ ($\rho = 10$). As can be observed, the results computed with the model do not match with the ones obtained by simulation. This fact was intentionally exploited to show that while for different parameterizations the model and the simulation results match, for the specific parameterization adopted in the validation scenario the CLT does not hold because the k_l values are too small. Consequently, (30) is not an accurate approximation and a large deviation of the P_C's model is observed. In this case, it would be better to adopt the non-Gaussian approach, because it leads to more accurate model results.

In Figure 5 we compare the probability of having enough energy accumulated in the harvester battery to transmit a packet (P_C). The probability was computed using (44), that is the non-Gaussian approach, for $L = 2$ ($\rho = 200$), $L = 4$ ($\rho = 100$), and $L = 40$ ($\rho = 10$). The simulated values are the same as depicted in Figure 4; that is, the considered scenario is the same. As can be observed, the results computed with the model do not match with the ones obtained by simulation for $L = 2$ and $L = 4$. However, if more annuli are used, the model accurately characterizes P_C, as is the case for $L = 40$ in the figure. This fact is due to the approximation of k_l and θ_l in (23) and (24), respectively. As the number of annuli (L) increases, E[I] and Var[I] in (23) and (24) become more accurate.

As can be observed, the results computed with the model for $L = 40$ are close to the ones obtained by simulation. Moreover, the probability of reaching a battery charging level equal

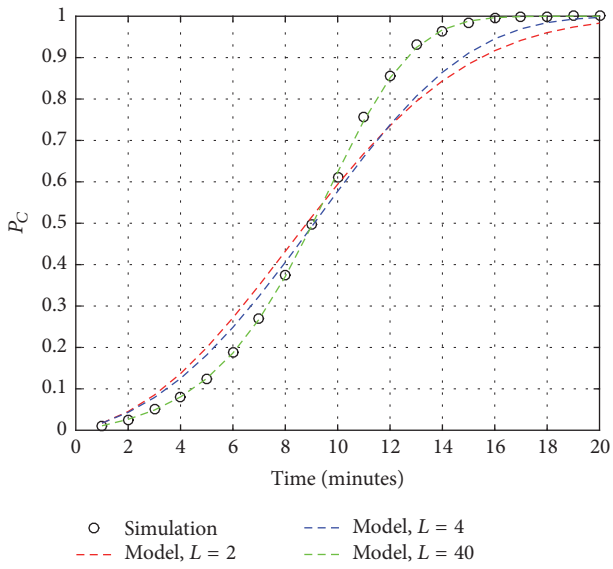

FIGURE 5: Non-Gaussian approach model: probability of having enough energy accumulated in the harvester battery to transmit a packet (P_C) for different density $\beta = 4 \times 10^{-4}$ of transmitters (β_l in nodes per square meter) located in the area $A = \pi((R_o^L)^2 - (R_i^1)^2)$.

to the γ threshold increases over time, as expected. The results confirm the accuracy of the proposed characterization, which may be easily adopted to evaluate the probability of charging over time.

Finally, we highlight that the mean aggregate RF power (I_{agg}) considered in the validation scenario is low to show the error of the Gaussian approach. For higher I_{agg} values, the error of the Gaussian approach becomes smaller and the model becomes more accurate. The non-Gaussian approach is generally a better solution (because it does not depend on the CLT); however it exhibits a higher computational complexity.

6. Final Remarks

In this paper we have characterized the battery charging time of a harvester node that accumulates the received RF energy in a battery. Admitting that the transmitters are spatially distributed according to a spatial Poisson process, we use the distribution of the received RF power from multiple transmitters to derive the probability of a harvester having enough energy to transmit a packet after a given amount of charging time. The distribution of the RF power and the probability of a harvester node having enough energy to transmit a packet are validated through simulation. The numerical results obtained with the proposed analysis are close to the ones obtained through simulation, which confirms the accuracy of the proposed analysis.

Competing Interests

The authors declare that they have no competing interests.

Acknowledgments

This work was partially supported by the Portuguese Science and Technology Foundation (FCT/MEC) under the project UID/EEA/50008/2013.

References

[1] T. Soyata, L. Copeland, and W. Heinzelman, "RF energy harvesting for embedded systems: a survey of tradeoffs and methodology," *IEEE Circuits and Systems Magazine*, vol. 16, no. 1, pp. 22–57, 2016.

[2] X. Lu, P. Wang, D. Niyato, D. I. Kim, and Z. Han, "Wireless networks with RF energy harvesting: a contemporary survey," *IEEE Communications Surveys and Tutorials*, vol. 17, no. 2, pp. 757–789, 2015.

[3] Y. Yao, J. Wu, Y. Shi, and F. F. Dai, "A fully integrated 900-MHz passive RFID transponder front end with novel zero-threshold RF-DC rectifier," *IEEE Transactions on Industrial Electronics*, vol. 56, no. 7, pp. 2317–2325, 2009.

[4] T. Salter, K. Choi, M. Peckerar, G. Metze, and N. Goldsman, "RF energy scavenging system utilising switched capacitor DC-DC converter," *Electronics Letters*, vol. 45, no. 7, pp. 374–376, 2009.

[5] G. Papotto, F. Carrara, and G. Palmisano, "A 90-nm CMOS threshold-compensated RF energy harvester," *IEEE Journal of Solid-State Circuits*, vol. 46, no. 9, pp. 1985–1997, 2011.

[6] S. Scorcioni, L. Larcher, A. Bertacchini, L. Vincetti, and M. Maini, "An integrated RF energy harvester for UHF wireless powering applications," in *Proceedings of the IEEE Wireless Power Transfer (WPT '13)*, pp. 92–95, IEEE, Perugia, Italy, May 2013.

[7] B. R. Franciscatto, V. Freitas, J. M. Duchamp, C. Defay, and T. P. Vuong, "High-efficiency rectifier circuit at 2.45 GHz for low-input-power RF energy harvesting," in *Proceedings of the European Microwave Conference (EuMC '13)*, pp. 507–510, IEEE, Nuremberg, Germany, October 2013.

[8] H. Ju and R. Zhang, "Throughput maximization in wireless powered communication networks," *IEEE Transactions on Wireless Communications*, vol. 13, no. 1, pp. 418–428, 2014.

[9] R. Zhang and C. K. Ho, "MIMO broadcasting for simultaneous wireless information and power transfer," *IEEE Transactions on Wireless Communications*, vol. 12, no. 5, pp. 1989–2001, 2013.

[10] X. Zhou, R. Zhang, and C. K. Ho, "Wireless information and power transfer: architecture design and rate-energy tradeoff," *IEEE Transactions on Communications*, vol. 61, no. 11, pp. 4754–4767, 2013.

[11] N. Pappas, J. Jeon, A. Ephremides, and A. Traganitis, "Optimal utilization of a cognitive shared channel with a rechargeable primary source node," *Journal of Communications and Networks*, vol. 14, no. 2, pp. 162–168, 2012.

[12] A. M. Ibrahim, O. Ercetin, and T. ElBatt, "Stability analysis of slotted aloha with opportunistic RF energy harvesting," *IEEE Journal on Selected Areas in Communications*, vol. 34, no. 5, pp. 1477–1490, 2016.

[13] A. Ghazanfari, H. Tabassum, and E. Hossain, "Ambient RF energy harvesting in ultra-dense small cell networks: performance and trade-offs," *IEEE Wireless Communications*, vol. 23, no. 2, pp. 38–45, 2016.

[14] X. Lu, I. Flint, D. Niyato, N. Privault, and P. Wang, "Self-sustainable communications with RF energy harvesting: ginibre point process modeling and analysis," *IEEE Journal on Selected Areas in Communications*, vol. 34, no. 5, pp. 1518–1535, 2016.

[15] X. Lu, P. Wang, D. Niyato, D. I. Kim, and Z. Han, "Wireless networks with rf energy harvesting: a contemporary survey," *IEEE Communications Surveys and Tutorials*, vol. 17, no. 2, pp. 757–789, 2015.

[16] L. Mohjazi, M. Dianati, G. K. Karagiannidis, S. Muhaidat, and M. Al-Qutayri, "RF-powered cognitive radio networks: technical challenges and limitations," *IEEE Communications Magazine*, vol. 53, no. 4, pp. 94–100, 2015.

[17] X. Lu, P. Wang, D. Niyato, and E. Hossain, "Dynamic spectrum access in cognitive radio networks with RF energy harvesting," *IEEE Wireless Communications*, vol. 21, no. 3, pp. 102–110, 2014.

[18] S. Lee, R. Zhang, and K. Huang, "Opportunistic wireless energy harvesting in cognitive radio networks," *IEEE Transactions on Wireless Communications*, vol. 12, no. 9, pp. 4788–4799, 2013.

[19] S. Khoshabi Nobar, K. Adli Mehr, and J. Musevi Niya, "RF-powered green cognitive radio networks: architecture and performance analysis," *IEEE Communications Letters*, vol. 20, no. 2, pp. 296–299, 2016.

[20] D. T. Hoang, D. Niyato, P. Wang, and D. I. Kim, "Opportunistic channel access and RF energy harvesting in cognitive radio networks," *IEEE Journal on Selected Areas in Communications*, vol. 32, no. 11, pp. 2039–2052, 2014.

[21] A. Bhowmick, S. D. Roy, and S. Kundu, "Throughput of a cognitive radio network with energy-harvesting based on primary user signal," *IEEE Wireless Communications Letters*, vol. 5, no. 2, pp. 136–139, 2016.

[22] A. H. Sakr and E. Hossain, "Cognitive and energy harvesting-based D2D communication in cellular networks: stochastic geometry modeling and analysis," *IEEE Transactions on Communications*, vol. 63, no. 5, pp. 1867–1880, 2015.

[23] A. Papoulis and S. U. Pillai, *Probability, Random Variables, and Stochastic Processes*, McGraw-Hill, New York, NY, USA, 4th edition, 2001.

[24] A. Abdi and M. Kaveh, "On the utility of gamma pdf in modeling shadow fading (slow fading)," in *Proceedings of the IEEE 49th Vehicular Technology Conference*, vol. 3, IEEE, Houston, Tex, USA, May 1999.

[25] S. Al-Ahmadi and H. Yanikomeroglu, "On the approximation of the generalized-κ distribution by a gamma distribution for modeling composite fading channels," *IEEE Transactions on Wireless Communications*, vol. 9, no. 2, pp. 706–713, 2010.

[26] M. Abramowitz and I. A. Stegun, *Handbook of Mathematical Functions with Formulas, Graphs, and Mathematical Tables*, Dover, New York, NY, USA, 1965.

[27] M. Haenggi and R. K. Ganti, *Interference in Large Wireless Networks*, Now Publishers Inc, 2009.

[28] A. M. Mathai, "Storage capacity of a dam with gamma type inputs," *Annals of the Institute of Statistical Mathematics*, vol. 34, no. 1, pp. 591–597, 1982.

[29] P. G. Moschopoulos, "The distribution of the sum of independent gamma random variables," *Annals of the Institute of Statistical Mathematics*, vol. 37, no. 1, pp. 541–544, 1985.

[30] N. L. Johnson and S. Kotz, *Continuous Univariate Distributions: Distributions in Statistics*, vol. 1, Houghton Mifflin, 1970.

[31] H. Tang, "Some physical layer issues of wide-band cognitive radio systems," in *Proceedings of the 1st IEEE International Symposium on New Frontiers in Dynamic Spectrum Access Networks (DySPAN '05)*, pp. 151–159, IEEE, Baltimore, Md, USA, November 2005.